Adaptive Effects of Spaceflight as Revealed by Short-Term Partial Weight Suspension

D. KEOKI JACKSON, SC.D., AND DAVA J. NEWMAN, PH.D.

JACKSON DK, NEWMAN DJ. *Adaptive effects of spaceflight as revealed by short-term partial weight suspension.* Aviat Space Environ Med 2000; 71(9, Suppl.):A151–60.

Background: Human performance and adaptation to altered loading levels is investigated. A previous astronaut jumping study demonstrated significantly altered landing performance following spaceflight, complementing reports of postflight postural and gait instabilities. A dynamic model indicated that leg stiffness changes accounted for the kinematic differences due to adaptation in open-loop modulation of leg impedance. Muscular atrophy or altered stretch reflexes and vestibular sensing could not be discounted. ***Hypothesis:*** We hypothesize that partial weight unloading can cause modulation of leg impedance and altered jump landing performance similar to longer-term microgravity exposure, while controlling for muscle atrophy and altered graviceptor inputs. Lower-body impedance changes after partial weight unloading support the hypothesis that postflight differences result primarily from modulation of leg impedance due to reduced postural control demands in microgravity. ***Methods:*** Six subjects performed six baseline 30-cm downward jumps from a platform, followed by 10 jumps under 60% body weight unloading (the adaptation sequence), and then six additional jumps under full-body loading (termed "adapted jumps"). Joint and mass center kinematics were compared for the baseline and adapted jump landings. A second order model evaluated changes in vertical leg impedance. ***Results:*** Three subjects exhibited significant increased joint angles and rates. Vertical ground reaction forces showed more heavily damped responses after adaptation. Model fits to mass center motion indicated reduced leg stiffness. ***Conclusions:*** Post-adaptation performance is similar to that of four astronaut subjects who demonstrated reduced postflight leg stiffness. The new study strongly suggests adaptive control of lower limb impedance to accommodate altered gravity levels which can be induced by minimal unloading exposure. Partial weight unloading provides a simple, inexpensive analog to spaceflight for certain postural and movement studies.

Keywords: spaceflight, partial gravity, microgravity, performance, adaptive control.

MANY STUDIES HAVE recorded changes in astronaut balance, posture, and motion control in the microgravity environment of spaceflight and following return to Earth's gravitational field. Abnormal postural sway and reduced stance stability were observed following spaceflight (7,9,20,28). Postflight locomotion disorders included deviations from straight paths, shift of the body toward the stance leg, stamping gait and abnormal head-trunk coordination (4,3). Anecdotal observations of wide stance during gait and difficulty rounding corners provide further evidence for degraded balance and locomotion after spaceflight (8).

Impact absorption in landing from falls or jumps also exhibits significant changes after microgravity exposure. Astronauts subjected to sudden falls were unsteady after spaceflight (25). A recent study evaluated the performance in two-footed jump landings of Space Shuttle astronauts before and after their shuttle missions (18). Of 9 subjects, 6 showed significant alterations in their leg joint and body mass center (CM) kinematics during impact absorption after return from space. Four demonstrated increased leg joint flexion and flexion rates, larger downward CM motion, and slower CM response trajectories. They were designated "Postflight-Compliant" (P-C) because the kinematic results indicated reduction in the net vertical stiffness provided by the legs. In contrast, two subjects were labeled "Postflight-Stiff" (P-S) because they exhibited reduced joint and CM deflections after spaceflight combined with lower peak joint rates.

Performance decrements in posture control and locomotion have been attributed to a range of microgravity-related effects on sensory interpretation, antigravity musculature, and neural feedback and processing. Control of gait and posture relies on integration of sensory signals including vestibular information, visual cues and limb proprioception. Human spaceflight studies have indicated central nervous system (CNS) reinterpretation of otolith signals and increased dependence on visual information (21,28). Reduced arm-pointing accuracy in blindfolded astronauts indicated impaired proprioception (24), as did reports by an astronaut performing a drop test stating that "he fell because his legs were always further forward than he expected" (25).

Atrophy of the antigravity muscles in the legs and altered tonic muscle activation patterns have been reported during spaceflight, and could contribute to postflight postural instability (6,12). Likewise, changes in CNS processing are likely to contribute to altered performance. The otolith-spinal reflex helps to prepare the leg musculature for impacts after sudden drops, and is dramatically reduced in microgravity, although normal function is recovered almost immediately on return to Earth (25). Microgravity-induced alterations in tendon stretch reflexes together with apparent reorganization of higher level anticipatory postural responses provide evidence for spaceflight adaptation in the feedback and

From the Lockheed Martin Missiles and Space, Sunnyvale, CA (D. K. Jackson); and Man-Vehicle Laboratory, Massachusetts Institute of Technology, Cambridge, MA (D. J. Newman).

Address reprint requests to: Dava J. Newman, Ph.D., who is an Associate Professor of Aeronautics and Astronautics, 77 Massachusetts Avenue, Room 33-407, Department of Aeronautics and Astronautics, Cambridge, MA 02139; dnewman@mit.ed

feedforward contributions of the CNS to postural control and movement (6,10).

The kinematic results of the astronaut jumping study suggested that leg impedance modulation accounted for the differences seen following spaceflight. On Earth, the body's inverted pendulum structure requires a minimum stiffness of the postural control system for stance stability. Stabilization against gravity is not required in spaceflight, allowing reduced limb stiffness and control bandwidth without postural instability. The P-C subjects demonstrated more heavily damped responses and reduced net stiffness postflight, suggesting aftereffects of reduced control bandwidth demands in flight. In contrast, the P-S subjects may have represented a strategy that recognized and overcompensated for this stiffness reduction in flight. Postflight overcompensation is consistent with a "rebound" in the potentiation of the H-reflex in some astronauts, and attempts by some subjects to control upright posture tightly within a narrow "cone of stability" (22,28).

Changes in leg impedance could result from reduced force-generating capability due to muscle atrophy or altered sensory feedback as discussed above. However, substantial evidence suggests that the effective impedance is set in an open-loop manner prior to impact through antagonist muscle coactivation and control of the limb configuration. Postflight changes in astronaut knee joint kinematics during gait provided additional evidence for joint impedance changes resulting from adaptation to weightlessness (13). Jumping studies of animals and humans show pre-programmed muscle activation patterns and joint motion timed for expected impact (5,14,23). The legs behave much like a constant stiffness spring in running (15), therefore, a simple second order model of the vertical leg impedance was used to evaluate astronaut jump landings, and showed that the postflight changes could be captured by varying the net vertical leg stiffness.

P-C astronaut data indicated that reduced demands on the postural control system in microgravity permitted reduction of the leg stiffness, altering the kinematics of the postflight jumps. Possible explanations for changes in leg impedance include altered central control of leg stiffness, postural muscle deconditioning, and changes in vestibular or stretch reflex feedback. Short term unloading of the leg anti-gravity muscles tests whether adaptive changes in leg impedance control occur as a consequence of reduced load bearing requirements. Muscle atrophy is not a concern in short, 2-min unloading adaptation periods. Moreover, vestibular sensing is unaffected during unloading in normal gravity. For these reasons, a test of jumping following short exposures to simulated partial gravity was devised to further investigate the astronaut results.

We hypothesize that short-term partial weight unloading (PW) can cause changes in jump landings that replicate key aspects of the postflight differences seen in astronauts, including changes in the net vertical stiffness of the legs. Furthermore, we hypothesize that postflight changes in astronaut jump landing performance resulted from adaptive open-loop modulation of leg impedance appropriate for the postural control requirements of microgravity.

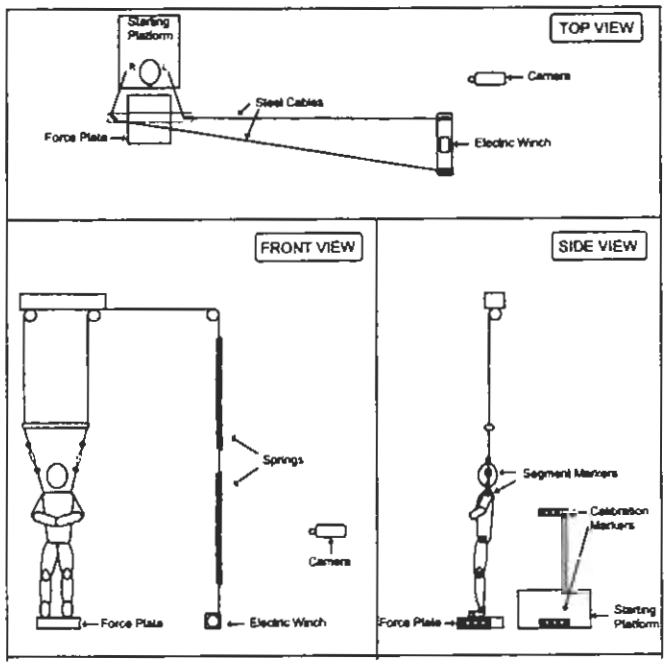

Fig. 1. Partial weight suspension system, or moonwalker, and jump platform. The subject is suspended by a harness attached to steel cables. Unloading is controlled by varying the spring tension with the electric winch. A video camera records the subject's left side with marker locations indicated in the side view.

METHODS

Experimental Apparatus

Fig. 1 shows the jump platform, force plate and suspension system, commonly referred to as the "moonwalker," used in the PW protocol. Subjects jumped 30 cm down from the platform onto the force plate. The PW apparatus uses an overhead suspension system to partially unload the legs. The subject wears a nylon harness (Mori Safety Products, Toronto, ON, Canada) with loops about each thigh that connect to shoulder straps. The leg loops applied the upward force at the inner thighs and buttocks. The straps applied smaller horizontal forces to the back and chest directed toward the suspension point. This horizontal component acted as a restoring force toward upright posture when the subject was directly beneath the overhead attachment, but otherwise pulled the subject away from an upright stance.

Each shoulder strap was connected to a steel cable that ran through overhead pulleys to a spring. A steel cable and electric winch controlled the spring stretch and hence the upward force exerted on the subject by the harness. The actual spring length varied with the subject's motion producing an additional upward force of ~80 N when the subject was standing on the force plate compared with the starting platform. The variation in upward force over the vertical span of the jump ranged from 12–16% of subject body weight. Unloading 60–100% of the subject's body weight caused the subject to lean about 12° farther forward than normal.

An AMTI OR6–5 force plate (Advanced Medical Technology, Inc., Newton, MA) measured ground reaction forces. Force signals were amplified and low-pass filtered with a corner frequency of 1050 Hz by an AMTI MCA amplifier, then sampled at 2000 Hz using a Power Macintosh 8100/80 computer equipped with a National Instruments NB-MIO-16 L data acquisition board.

Body segments on the left side of the subject were tracked using a single Sony Handycam 8 mm camcorder to record the position of six markers placed at the toe, ankle, knee, hip, shoulder and ear. The markers were placed at: 1) the fifth toe metatarsal-phalangeal joint; 2) the lateral malleolus; 3) the lateral femoral epicondyle; 4) the greater trochanter of the femur; 5) the acromian process; and 6) the center of the ear.

The subjects wore skintight black stockings on the legs and left arm, and a black form-fitting cap covered the ear. White labels measuring 2.5 cm x 1.9 cm provided excellent marker contrast against the black background. Double-sided tape secured the stockings to the skin over the areas of interest. Additional calibration markers were fixed within the camera field-of-view. A mapping of the true spatial coordinates to the camera focal plane coordinates was derived using an array of calibration markers. The video frames were digitized in 8 bit gray-scale at a rate of 30 frames per second with a resolution of 280 pixels vertically and 320 pixels horizontally using the built-in Power Macintosh 8500 video card and the Adobe Premiere software package. A LabView program was written to threshold the images and extracts the centroid of each individual marker with respect to the frame. The mapping obtained from the calibration marker array was applied to correct for distortions in the image. Further errors were introduced by variations in marker distance from the camera for positions not directly aligned with the viewing axis of the camera, thus, the marker location in the sagittal plane was corrected for the estimated distance of the marker from the camera. The average measurement resolution was better than 3 mm over the camera field of view, ranging from 2.4 mm in the center of the image to 4.5 mm near the edges.

Experimental Protocol

The experimental protocol was approved for use with human subjects by MIT's Committee on the Use of Humans as Experimental Subjects (COUHES). All subjects provided informed consent. The six volunteer female subjects were between 22 and 27 yr old, with heights and weights ranging from 160–173 cm and 52–71 kg. All subjects were athletic and in good health. Each subject performed two ataxia tests to screen for potential vestibular defects: 1) quiet standing with eyes closed in the sharpened Romberg stance; and 2) walking a line with the eyes closed (6). All subjects met the criteria for vestibular normals.

Before beginning the experiment, the lateral dimensions of the subject's body with the feet together were measured at the marker locations. The subject donned the suspension harness, which was initially detached from the suspension cables. Before the initial baseline jump, the subject stood with the toes at the edge of the starting block, and the feet were aligned on either side of an 8.9 cm wide wooden block to be parallel and facing straight ahead. The outer edge of each foot was marked on the block, and the subject placed her feet in the same position before each jump.

The subject performed 6 baseline jumps with the arms folded across the abdomen, so that one hand gripped the opposite wrist. The subject was instructed to: 1) look down at the landing platform before jumping; 2) perform a two-footed downward jump, taking off and landing with both feet simultaneously; and 3) recover to an upright standing position at a comfortable pace, and look straight ahead. The command to the subject for each jump was: "Look down. One, two, ready, jump." After the subject returned to an upright stance, the inter-ankle distance and the position of the fifth toe and lateral malleolus of the left foot were measured. These measurements were used together with the subject lateral body dimensions to estimate marker positions along the direction parallel to the camera axis in the video processing.

After the baseline jumps, the subject repeated the following sequence 6 times: 1) 10 jumps under 60% body weight unloading; then 2) 1 jump with no unloading. For the unloaded jumps, the harness was attached to the overhead suspension cables and the winch was used to stretch the springs until the force plate output read 40% of the subject's body weight. No data were taken during the unloaded jumps, but the subject instructions were the same as in the baseline sequence.

After the tenth adaptation jump, the subject was quickly prepared to make a single jump while supporting her full-body weight. The subject stepped up onto the starting platform, the spring tension was released and the cables were detached. The jump was performed using the baseline procedure. Preparation steps following the final unloaded jump were performed as quickly as possible to minimize the time the subject might readapt to the normal loading condition.

Data Analysis

The ankle, knee and hip joint angles in the left leg were computed using the positions of the markers at the toe, ankle, knee, hip and shoulder (**Fig. 2**). These calculations assumed that the foot, shank, thigh and trunk were rigid segments. Average resting joint angles during quiet standing were calculated and subtracted from the joint angle time series data. Positive joint angles indicated increased flexion from the rest position. Joint angular velocities were found by numerically differentiating the joint angle data using a four point centered difference. Before differentiating, angle data were smoothed by filtering forward and backward (to eliminate phase shift) using a third order Butterworth filter with a corner frequency of 7.5 Hz. Ground impact resulted in large and nearly instantaneous increases in the joint angular velocities. In order to avoid excessive smoothing of this feature, the data segments prior to and following impact were filtered and differentiated separately.

Impact time was determined from the discontinuity in the downward velocity of the toe marker. For each

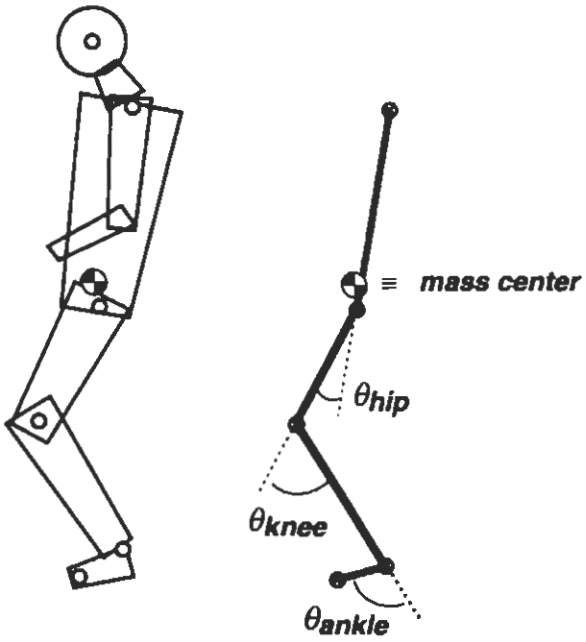

Fig. 2. Sagittal plane body model. Marker placement (denoted by "o") and eight segments used for body mass center (CM) calculation (feet, shanks, thighs, trunk, forearms, upper arms, neck and head) are shown at left. The joint angle convention is shown at right.

jump, peak flexion angles and flexion rates after impact were computed for the ankle, knee and hip joints. The position of the full-body CM in the sagittal plane was estimated from the marker positions, using an 8-segment body model (feet, shanks, thighs, trunk, upper arms, forearms, neck and head). Lateral symmetry was assumed, allowing combination of the left and right segments in the arms and legs. The arms were assumed to remain crossed in a fixed position relative to the trunk. The approximate body segment mass distribution was found using a regression model based on the subject's weight and height (27). The velocity of the CM was found using the same numerical differentiation procedure described above for the joint angular velocities. The positive vertical direction was upward.

Initial analysis of the joint and CM kinematics indicated a non-uniform pattern of responses across the subject pool. Therefore, baseline and adapted data sets were compared for each subject individually for peak joint flexion angles, peak joint flexion rates, and CM-related measures. Student's *t*-tests were used to compare the baseline and post-adaptation data sets. Tests yielding $p < 0.05$ were considered statistically significant.

Changes from baseline to post-adaptation jumps in five measures were considered for classification of the subjects into groups. These measures were previously selected for classification purposes in the astronaut jumping study because they proved relatively insensitive to day-to-day variations in preflight testing (18). The five variables were tested together for the effects of test session using a multivariate analysis of variance (MANOVA). The contrast for adaptation effect was computed for baseline vs. post-adaptation data sets. Probabilities were based on Wilks' Lambda (likelihood ratio criterion) and Rao's corresponding approximate (sometimes exact) F-statistic. Subjects who did not exhibit significant differences between baseline and post-adaptation for the multivariate measure were classified as "No Change" (N-C).

Other subjects could be classified as either "Post-adaptation Compliant" (P-C) or "Post-adaptation Stiff" (P-S) by scoring the five individual measures used in the MANOVA. These designations corresponded to the Postflight Compliant and Postflight Stiff classifications in the astronaut study. For each measure, the subject received a +1 for a significant change toward greater compliance after adaptation, a −1 for a significant change toward lower compliance after adaptation, and a 0 for no significant change. The results for the individual measures were summed to get an overall score ranging from −5 to +5. Subjects with positive scores were designated P-C, while negative scores were labeled P-S. All statistical computations were performed using SYSTAT (26).

Model of CM Vertical Motion

A simple mechanical body model was developed to investigate the vertical motion of the CM following impact with the ground. In this single degree-of-freedom model horizontal motion was neglected (**Fig. 3**). The entire body mass was concentrated at the CM, supported by a massless, constant stiffness linear spring representing the legs. Similar models have been used to examine hopping and running (1,15). The upward restoring force exerted by the spring was proportional to the downward displacement of the CM from the uncompressed spring length Z_o (nominally the height of the CM at the moment of impact). Energy dissipation, or damping, was modeled by a linear dashpot in parallel with the leg spring that opposed the CM motion with a force proportional to CM velocity.

This model led to a second order linear differential equation that described the CM motion:

$$M\ddot{z} + B\dot{z} + K(z - Z_o) = Mg \qquad \text{Eq. 1}$$

$$\ddot{z} + \frac{B}{M}\dot{z} + \frac{K}{M}(z - Z_o) = g \qquad \text{Eq. 2}$$

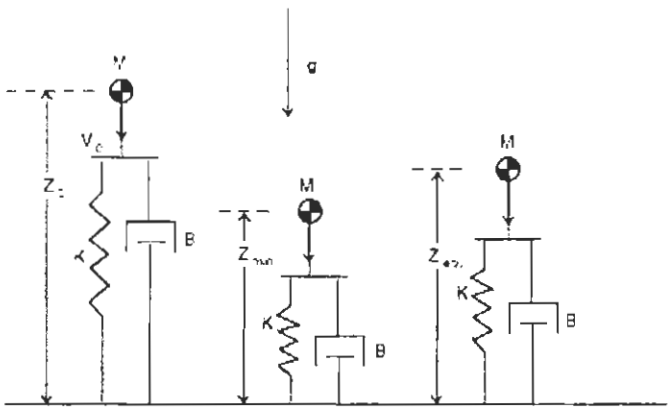

Fig. 3. Second order model of CM vertical (Z) motion following impact. Body mass (M), located at the CM, is supported by linear spring (K) and dashpot (B). The unloaded length of the spring is Z_o (nominally the height of the CM at impact), minimum spring length is Z_{min}, and the spring length at the final equilibrium is Z_{equil}.

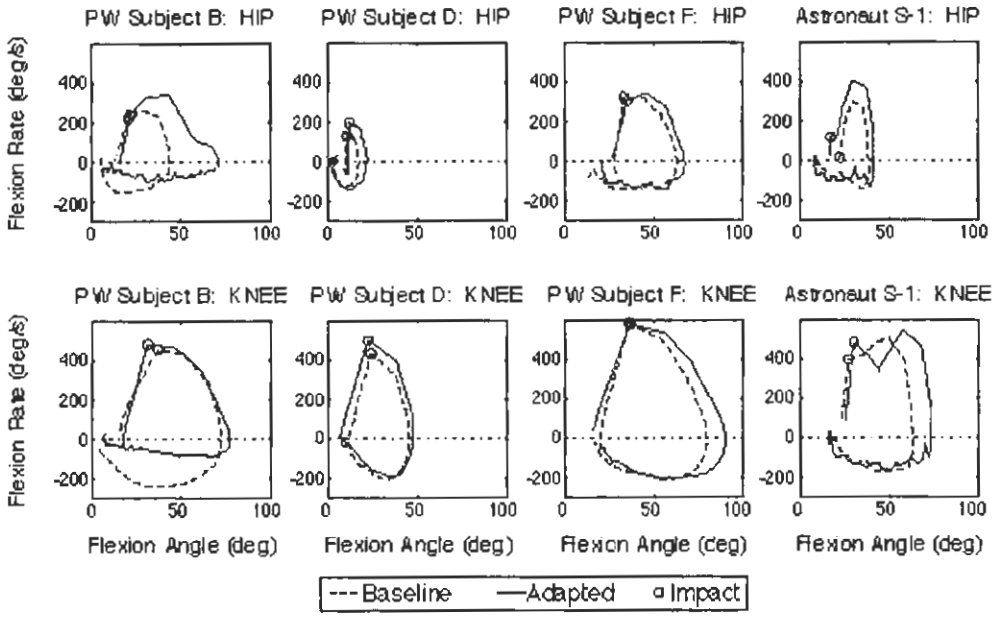

Fig. 4. Baseline and adapted joint phase-plane portraits for three partial weight unloading (PW) subjects and one astronaut subject. Each trace represents the average of 6 trials. Trials are aligned at impact (denoted by the open circle, o). Phase-plane portraits are traversed in the clockwise direction.

where z, zdot, z double dot = CM vertical position, velocity, and acceleration, respectively; g = gravitational acceleration, M = body mass, K = spring stiffness, B = damping.

The vertical position and velocity of the CM gave the initial conditions necessary to find the time solution of the equations at the moment of impact. In order to compare the pre- and postflight limb impedance properties for each subject, best fit values for each jump trajectory were determined for the stiffness and damping coefficients using the MatLab System Identification Toolbox (The MathWorks Inc., Natick, MA). Model fitting was accomplished by minimizing a quadratic prediction error criterion using an iterative Gauss-Newton algorithm (11). The best fit for the rest spring length Z_o was determined concurrently, although this parameter is nominally set by the height of the CM at impact. Unfortunately, the 30 Hz sampling rate was too low to provide an adequate estimate of the Z_o value. With CM velocities greater than 2 $m \cdot s^{-1}$ at impact, an uncertainty of one sampling interval in the time of impact could result in errors in Z_o exceeding 6 cm. Since peak deflection of the CM following impact typically ranged from 8–15 cm, this level of uncertainty required simultaneous estimation of the rest length.

Eq. 2 was rewritten in canonical second order form as:

$$\ddot{z} + 2\zeta\omega_n\dot{z} + \omega_n^2(z - Z_0) = g \qquad \text{Eq. 3}$$

where $\omega_n = \sqrt{\frac{K}{M}}$ = natural frequency.

The natural frequency was roughly equivalent to the bandwidth of the system and provided a measure of the speed of response, since higher natural frequencies corresponded to faster transient responses. Increasing the stiffness K led to a higher natural frequency. The damping ratio measured how oscillatory the transient response was, with lower damping ratios indicating more overshoot and oscillation in the system behavior. Decreasing the stiffness K increased the damping ratio.

RESULTS

Jump Landing Kinematics

Phase-plane plots for the leg joints provided a convenient graphical method for comparing the angles and rates in the baseline and PW-adapted jump landings. The results of the astronaut study indicated that exposure to spaceflight most consistently affected knee and hip joint kinematics in jump landings. **Fig. 4** shows phase-plane plots of hip and knee joint trajectories for the three subjects (B, D, F) who exhibited significant changes in peak flexion or flexion rate at these joints. These baseline and post-adaptation phase portraits were constructed by synchronizing each set of trials at the time of impact, then averaging the joint angles and rates at each individual sample. The plots are traversed clockwise in time from the moment of impact (marked with an open circle). Peak joint flexion rates occur within one or two samples of impact at the uppermost point on the plots. The maximum joint flexion is reached at the far right of the graph when the joint rate is zero. Joint extension is observed in the negative rates at the bottom of the plot as the subject recovers to an upright stance.

These three PW subjects show general post-adaptation increases in peak knee and hip deflection, as well as greater maximum hip flexion rates after impact. Also noteworthy is the substantial decrease in the peak extensional joint rates for subject B, which corresponds to the much slower return to upright equilibrium after PW adaptation. The P-C astronaut subjects demonstrate very similar kinematic characteristics, and a represen-

TABLE I. MAXIMUM AVERAGE (A) KNEE AND (B) HIP JOINT FLEXION ANGLES AFTER IMPACT SHOWING THE ANGLE, STANDARD ERROR OF MEAN (SEM) AND THE DIFFERENCE BETWEEN BASELINE AND PW ADAPTED (MEAN DIFF).

	Baseline (°)		Partial Weight Adapted		Change (°)	
Subject	Mean	SEM	Mean	SEM	Mean Diff	p-Value
A. Maximum Knee Angle						
A	78.4	0.8	81.6	1.5	3.2	0.084
B	73.0	1.0	77.3	1.3	4.4	**0.025**
C	54.9	1.0	54.8	1.4	−0.2	0.921
D	46.6	0.6	47.9	1.4	1.3	0.415
E	72.3	1.6	73.1	1.8	0.8	0.743
F	80.2	1.1	90.4	0.6	10.2	0.000
All Subjects	67.7	2.2	70.3	2.6	2.6	0.449
B. Maximum Hip Angle						
A	62.1	2.2	62.4	2.9	0.3	0.938
B	44.0	1.8	72.0	4.4	28.0	**0.000**
C	24.5	1.9	30.0	2.4	5.5	0.100
D	18.7	1.0	22.1	1.0	3.4	**0.040**
E	64.7	3.0	61.7	3.5	−3.0	0.548
F	64.6	2.6	67.9	1.6	3.2	0.340
All Subjects	46.4	3.3	52.3	3.5	5.9	0.224

tative astronaut's phase-plane portrait is included for comparison.

Table I shows maximum knee and hip flexion angles for each subject for the baseline and PW-adapted jumps. Three of the subjects exhibit significant increases ($p < 0.05$, Student's t-test) in maximum flexion at one or more joints. No significant decreases in peak joint flexion were observed at any joint in any subject. No significant changes were found with all subjects grouped together.

Subject B exhibits a significant average increase in peak knee flexion of approximately 5°, combined with a significant increase of nearly 30° in peak hip flexion. Subject F demonstrates a significant increase in maximum knee flexion of 10° after unloading exposure, while a significant increase of about 3° in peak hip angle was noted for subject D.

Subject Classification

The joint angle phase diagrams suggested that the PW subjects could be classified in the same manner as the astronauts. Using the analogy of a spring of variable stiffness, the first group was denoted "post-adaptation compliant", or P-C. Just as a more compliant spring compresses more under a given load, this group generally exhibited greater joint flexion after adaptation, accompanied by increased flexion rates. Subjects with an opposite response would be labeled "post-adaptation stiff," indicating lower peak flexion and flexion rates for the jump landings after PW exposure.

The CM kinematics provided complementary information for classification of subject performance following adaptation. If the legs were considered to be roughly springlike in supporting the mass of the upper body, the maximum downward deflection of the CM following impact gave a measure of the stiffness of the lower limb "spring" (e.g., an increase in the downward deflection of the mass center indicated a decrease in spring stiffness). The time from impact to the point of peak downward deflection also provided an indicator of the effective stiffness of the lower limbs. A decrease in the time between impact and maximum deflection implied an increase in the stiffness.

Table II scores the five measures used to classify each subject. Positive entries indicate significant changes toward greater compliance post-adaptation, corresponding to increases in peak joint angles or peak joint flexion rates, greater downward CM deflection, or longer times from impact to maximum CM vertical deflection. Negative entries would represent significant differences in these quantities, indicating greater stiffness after adaptation, although no such measurements were recorded. The statistical significance for the preflight/postflight MANOVA contrast of the five measures is shown for each subject (p-value). As previously mentioned, subjects with significant MANOVA results were denoted P-C or P-S based on positive or negative overall scores respectively for the five classification measures; the remainder are designated "No Change" (N-C).

Three subjects (B, D and F) were classified P-C. As discussed above, all three have significantly increased peak flexion at the hip or knee, although only peak knee flexion is evaluated in the MANOVA. In addition, subjects B and D exhibit significantly increased peak hip flexion rate. Subjects B and F demonstrate greater downward CM deflection after adaptation, while subject B also shows an increase in the time to maximum CM deflection. The remaining three subjects (A, C and E) show no significant changes in the individual measures, and are designated N-C based on lack of statistical significance in the multivariate criterion. No subjects demonstrate P-S characteristics.

Vertical Ground Reaction Forces

Fig. 5 shows force plate results for subject B as a representative graph. The vertical ground reaction force (GRF) traces superimpose the baseline and post-adaptation averages. All data were aligned at time of impact, which is the origin of the time axis. Two trends in the

TABLE II. SUBJECT CLASSIFICATION BASED ON 5 KINEMATIC MEASURES AND PRE- AND POST-ADAPTATION RESULTS MANOVA COMPARISONS.

	Subjects					
	A	B	C	D	E	F
1. Peak Knee Flexion		+1				+1
2. Peak Knee Flexion Rate						
3. Peak Hip Flexion Rate		+1		+1		
4. Peak CM Deflection		+1				+1
5. Time to Peak CM Deflection		+1				
Overall Score	4	+4	0	+1	0	+2
p-value	0.742	**0.006**	0.805	**0.017**	0.404	**0.003**
Classification	N-C	**P-C**	N-C	**P-C**	N-C	**P-C**

Positive numbers indicate reduced stiffness after adaptation.
Classifications are no change (N-C) or partial weight adaptation compliant (P-C).

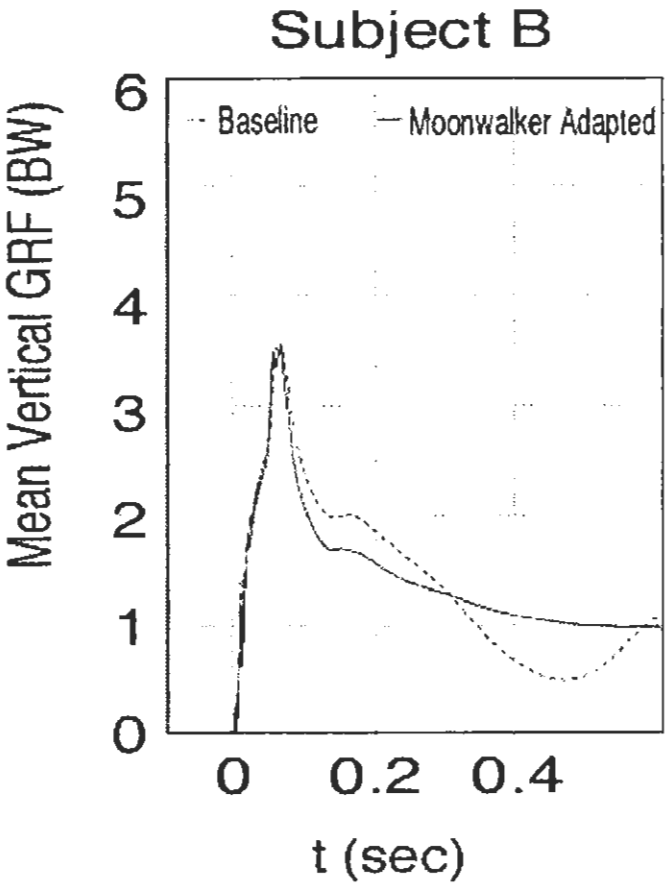

Fig. 5. Example of vertical ground reaction force (GRF) traces for PW subject B. Baseline and post-adaptation averages. Trials aligned at impact, shown at $t = 0$.

force data are apparent. First, the force traces for the adapted jumps tend to lag behind the forces from the baseline jumps. This effect is most easily observed by comparing the times when the ground reaction force decreases below the 1 body weight level. At this moment during the recovery toward upright posture after landing, the mass center was no longer being accelerated upward. This figure also shows that the minimum ground reaction force generally increases in the adapted jumps, compared with the minimum level seen in the baseline jumps. The minimum force level occurs during the portion of the recovery period when the mass center was moving upward toward the standing posture while being decelerated to a state of zero vertical velocity. The minimum vertical ground reaction force, or force undershoot, is used to quantify the system's oscillatory behavior.

In order to quantify the lag in the force traces for the adapted jumps, the time after impact when the vertical GRF falls below 1 body weight is computed for each jump. **Fig. 6** shows the timing data for all six subjects. The average time to the body weight crossover point is shown to increase after unloading adaptation for all subjects. Using an unpaired, two-tailed Student's *t*-test, this effect was significant at the $p < 0.05$ level for subjects B, D and F, as well as for all subjects grouped together. Hence, a general pattern of slower recovery

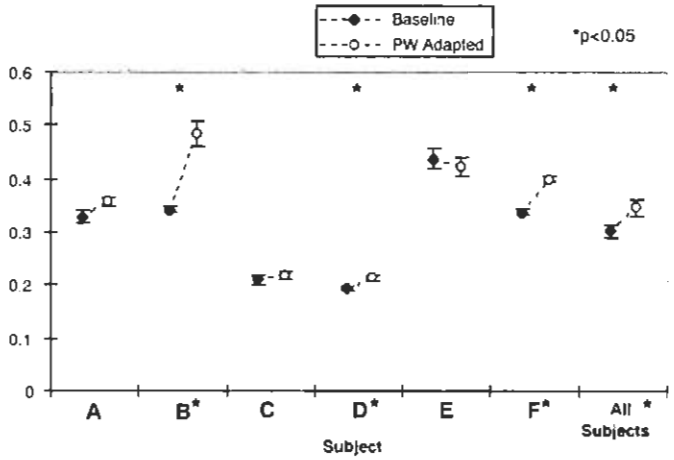

Fig. 6. The time interval for the vertical GRF from the moment of impact to a level of 1 body weight. Error bars indicate ± 1 standard error of the mean (SEM).

after unloading adaptation was indicated by the force plate data.

A similar comparison of the minimum vertical GRF is presented in **Fig. 7**. In this case, the average value of minimum GRF increased for each subject following unloading with the moonwalker. The increases were significant ($p < 0.05$, Student's *t*-test) for subjects B, D and E, and for the data of all subjects grouped together. This reduction in undershoot below the final 1 body weight value suggested that the system became less oscillatory after exposure to simulated partial gravity.

Second Order, Single Degree of Freedom Model of Vertical CM Motion

Linear leg stiffness and damping values were fit to the CM data for each jump using the mechanical model described above. **Fig. 8** shows predicted CM model responses using parameters estimated for representative P-C subject B. Model fits for the 6 baseline (Fig. 8a upper) and 6 post-adaptation (Fig. 8a lower) trials are staggered along the vertical axis. Fig. 8b shows baseline (upper) and post-adaptation (lower) average CM vertical trajectories; the shaded region indicates ± 1 SD. Simulated model results using the pre- and post-adap-

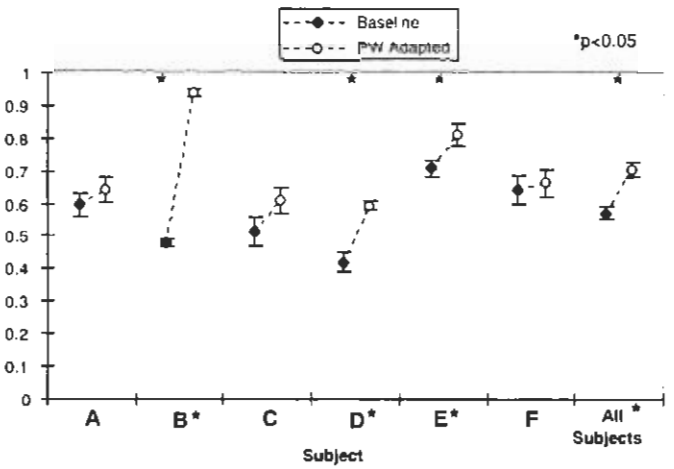

Fig. 7. Vertical GRF minimum value. Error bars indicate ± 1 SEM.

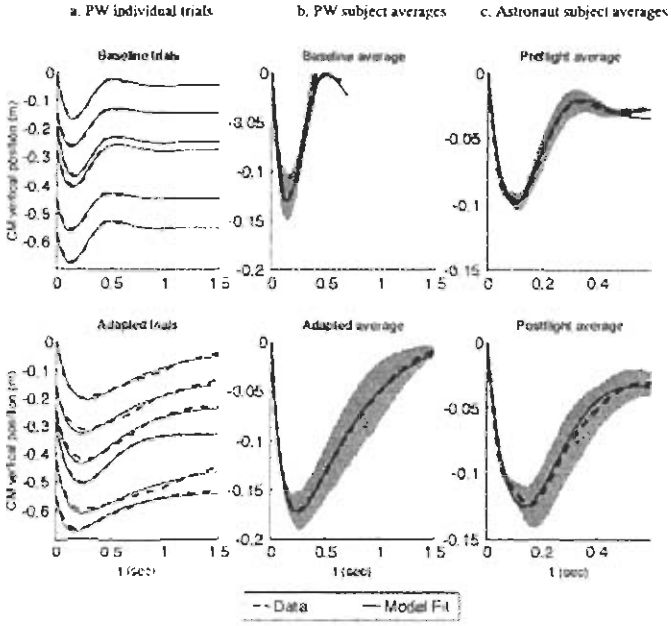

Fig. 8. Modeled CM vertical trajectory for representative subject B. CM motion is simulated using estimated stiffness and damping. Dashed lines are experimental data and solid lines represent model fits. (a) Left plots: 6 individual baseline trials (upper) and 6 post-adaptation trials (lower). (b) Center plots: Corresponding averages for trials shown in (a). Trials are synchronized at impact, shown as $t = 0$. (c) Right plots: Preflight and postflight averages for astronaut subject S-1. Shaded areas denote ± 1 SD.

tation stiffness and damping averages are included as well. The CM overshoot above the final equilibrium posture indicates a fairly low baseline damping ratio. The post-adaptation jumps show a much slower response with no overshoot. Thus, the adapted responses reflect a decreased natural frequency and increased damping ratio compared with the baseline jumps. For comparison, the pre- and post-flight average responses are included in Fig. 8c for P-C astronaut subject S-1. The postflight changes were very similar to the post-adaptation results of the moonwalker subject.

Average stiffness values for the baseline and adapted jumps are presented in **Fig. 9.** Individual subject base-

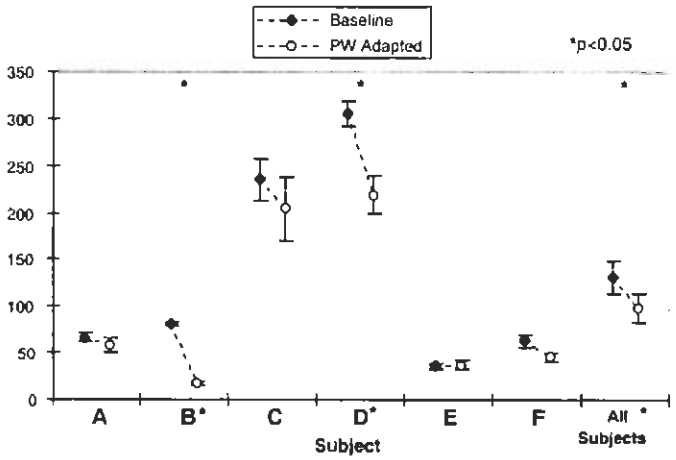

Fig. 9. Modeled stiffness estimates for all subjects. Error bars indicate ± 1 SEM. Statistical significance is from *t*-tests for individual subjects and ANOVA for grouped subject analysis.

TABLE III. MODULED NATURAL FREQUENCY AND DAMPING RATIO. (A) NATURAL FREQUENCY AND (B) DAMPING RATIO.

	Baseline		Partial Weight Adapted		Change	
Subject	Mean	SEM	Mean	SEM	Mean Diff	p-Value
A. Natural Frequency (rad · s^{-1})						
A	8.13	0.26	7.55	0.56	−7%	0.342
B	9.00	0.11	4.11	0.31	−54%	**0.000**
C	15.25	0.76	14.10	1.15	−8%	0.414
D	17.46	0.37	14.72	0.71	−16%	**0.007**
E	6.01	0.26	6.09	0.32	1%	0.863
F	7.89	0.42	6.72	0.38	−15%	0.087
All Subjects	10.68	0.72	8.94	0.78	−16%	**0.000***
B. Damping Ratio						
A	0.573	0.043	0.619	0.083	8%	0.623
B	0.514	0.014	1.195	0.099	132%	**0.000**
C	0.553	0.046	0.603	0.044	9%	0.450
D	0.539	0.049	0.713	0.027	32%	**0.012**
E	0.792	0.055	0.854	0.065	8%	0.486
F	0.498	0.047	0.558	0.048	12%	0.416
All Subjects	0.572	0.023	0.771	0.048	35%	**0.000***

* Indicates p-value from ANOVA for grouped subject analysis.

line and adapted parameter means are compared using an unpaired Student's *t*-test. This plot shows that the average leg stiffness decreases following partial weight unloading exposure in 5 of the 6 subjects. The decrease in stiffness is significant for all subjects grouped using a two-way ANOVA with subject and condition (baseline or adapted) as the independent variables. Significant effects of subject and interaction between subject and condition are also noted.

Of the 5 subjects with reduced stiffness, B and D demonstrate significant decreases of 79% and 28%, respectively, for the adapted jumps. Subject F shows a 28% decrease in average stiffness following adaptation, although this change was not significant ($p = 0.079$). The lack of statistical significance is attributed to a reduced number of data points, as the CM trajectories in two of her jumps were unavailable because the shoulder marker went beyond the camera field. However, subject F's stiffness decrease complements the significant changes observed for this subject in GRF traces and peak knee flexion after exposure to partial weight unloading. No significant changes are found in any subjects for the damping parameter in the model.

From the stiffness and damping coefficients, the natural frequency and damping ratio are calculated for each jump and presented in **Table III.** Increases in damping ratio from 8–132% are seen in all subjects. Subjects B and D exhibit significant damping ratio increases that reflect lower stiffness after moonwalker adaptation. The decrease in natural frequency and increase in damping ratio are significant for all subjects grouped together based on the two-way ANOVA. Significant effects of subject and the interaction between subject and condition are seen as well.

CONCLUSIONS

The results of the astronaut experiment suggested that gravity plays an important role in determining

stiffness levels selected by the neuromuscular system. Partial gravity simulation through suspension reduces the load-bearing demands on the legs and increases the body's inverted pendulum time constant. The required authority of the postural control system in reduced gravity therefore lies somewhere between the requirements for 1 G and weightlessness. Changes observed as a result of unloading exposure provide additional insight into the sometimes dramatic alterations observed in astronaut performance postflight.

The moonwalker experiments demonstrate that acute exposure to partial weight unloading can induce adaptive changes in jump landings. While PW is believed to provide a ground-based analog to microgravity exposure, the differences from the astronauts' experience must be considered. The upward forces exerted by the suspension system reduce the load-bearing requirements placed on the legs in a rough approximation of the effects of lower gravity. However, there are no changes in the gravitational forces on the otoliths, and the moonwalker suspension system also exerts forces on the body that are not comparable to true partial gravity. The upward force is applied locally by the harness, but the gravitational forces on the distributed mass of the body segments are unchanged. In addition, the actual upward force on the subject varies somewhat over the vertical range of motion. The net horizontal force while partially unloaded tends to cause a forward-leaning posture prior to jumping, and acts as a restoring force directed toward upright stance when the subject lands under the pulleys. The stable posture with the subject fully suspended contrasts with the neutrally stable rotational orientation of the subject during the normal free fall portion of a jump.

The effects that these differences may produce in comparison to true partial gravity are difficult to assess. However, PW provided an effective means of reducing the vertical load-bearing requirements on the legs, and permitted testing of the hypothesis that reduced demands on the postural control system can induce adaptive changes in the system stiffness and jumping kinematics. Furthermore, the load-bearing changes were not complicated by muscle atrophy or altered otolith inputs associated with microgravity.

Of course, substantial differences in adaptation stimuli, exposure durations and readaptation periods exist between the PW and astronaut experiments. Hence, the degree of similarity between the P-C responses in the two subject groups is remarkable. Half of the PW subjects exhibit significant post-adaptation increases in peak knee leg flexion angles similar to the peak joint angle increases observed the P-C group of astronaut subjects. None of the PW subjects demonstrate decreased peak joint flexion comparable to the P-S astronauts. The PW joint angle results are supplemented by force plate records in the moonwalker experiment that reinforce the similarities of these 3 subjects with the P-C astronaut group. Slower, less oscillatory vertical ground reaction responses in the PW adapted force plate data indicate a more heavily damped response following suspension, and are consistent with a general reduction of the leg stiffness. Hence, the aggregate data indicate that 3 of the 6 moonwalker subjects show results similar to those observed in P-C astronauts, while none exhibit characteristics like those of the P-S astronauts.

Like the astronaut postflight effects, the changes following exposure to simulated partial gravity are best explained by alterations in the controlled leg stiffness. Neither muscle atrophy nor changes in vestibular sensing can account for the moonwalker results. Sensory feedback latencies of 80–100 ms or more are comparable to the 100 ms duration of the entire impact absorption phase from landing to maximum joint flexion, eliminating the effect of post-impact sensory feedback on the majority of this portion of the jump landing (2,16,17). Furthermore, short term exposure to PW unloading using a similar protocol had no effect on patellar tendon reflexes (19).

The fact that a targeted unloading adaptation stimulus can replicate the effects of spaceflights lasting 1–2 wk is very interesting. These results indicate that the postural control system can tune stiffness quickly to account for variations in load bearing or the gravitational environment. In other short term unloading experiments, significantly increased RMS sway in most subjects' postural stabilograms coupled with reports of a temporary feeling of leg weakness, further supports the notion that PW can have significant effects on motor behavior (19). An optimal estimator model of postural control explained the effect through a decrease in ankle joint feedback gains, attributed to adaptive CNS-moderated decreases in muscular gains. This gain change is strikingly similar to the stiffness reductions exhibited by the P-C astronauts and PW jumping subjects, backing the hypothesis that microgravity and simulated hypogravity result in adaptive changes in the stiffness of the leg system.

The assumption that joint impedance characteristics transform into lumped leg stiffness and damping parameters governing the vertical CM motion following impact provides the basis for the second order mechanical model postulated herein. A similar model for running (15) and the generally close fits to experimental data obtained for the jumps in the astronaut and PW studies support the simplifying assumptions of constant stiffness and damping. Comparison of the astronaut pre- and postflight fits for this model indicate that lumped stiffness changes govern the differences in transient response observed on return to Earth. Likewise, the changes in joint kinematics and force plate data following PW exposure correlate well with the reduced stiffness estimates.

In the model, decreases in leg stiffness lead to decreases in bandwidth, with slower and less oscillatory time responses. Interestingly, the PW model fits do not show changes in the leg damping to play a role in the post-adaptation differences. This result is counterintuitive, since decreased limb stiffness through reduced antagonist muscle coactivation might be expected to cause a corresponding damping reduction. Furthermore, changes in damping in accordance with increases or decreases in stiffness would help to prevent large deviations in the damping ratio (see Eq. 3), which is often desirable from a control system standpoint. Re-

gardless, both PW and astronaut results indicate that independent modulation of limb damping and stiffness is possible, or simply that the damping characteristics are largely constant in the face of large changes in leg stiffness.

The limitations on the sensory feedback pathways indicate that the stiffness properties of the lower limbs are largely determined before impact. Hence, the changes in the model parameters corresponding to altered joint and mass center kinematics observed after adaptation are likely due to changes in the preprogrammed muscle activity prior to impact, which sets the limb impedance in an open-loop fashion by controlling the muscle tension-length properties and the limb configuration. This is the case for both the PW subjects and astronauts.

In summary, the astronaut study provided evidence for adjustment of lower limb impedance in response to spaceflight microgravity exposure. The PW experiment strengthened the conjecture that reduced postural demands in spaceflight contribute most to altered performance postflight. The PW protocol reduces the effective stiffness required of the postural control system, but is not believed to affect stretch reflexes, descending vestibular effects on muscle tone, or interpretation of vestibular acceleration signals. Hence, the significant changes seen after PW and microgravity adaptation most likely resulted from altered open-loop modulation of the limb trajectories and stiffness during the flight and impact phases of the jumps.

ACKNOWLEDGMENTS

The authors would like to thank the subjects who graciously performed these experiments. The authors wish to acknowledge their collaborators at the University of Pennsylvania, Professors Norm Badler and Dimitri Metaxas, and funding provided for this study in part by NASA grant NAG5-4928 and NAG5-3990.

REFERENCES

1. Alexander RM, Vernon A. Mechanics of hopping by kangaroos (Macropodidae). J Zoology 1975; 177:265–303.
2. Allum J, Pfaltz C. Visual and vestibular contributions to pitch sway stabilization in the ankle muscles of normals and patients with bilateral peripheral vestibular deficits. Exp Brain Res 1985; 58:82–94.
3. Bloomberg J, Reschke M, Huebner W, Peters B. The effects of target distance on eye and head movement during locomotion. Ann N Y Acad Sci 1992; 656(Sensing and Controlling Motion): 699–707.
4. Chekirda IF, Bogdashevskiy AV, Yeremin AV, Kolosov IA. Coordination structure of walking of Soyuz-9 crew members before and after flight. Kosmicheskaya Biologiya i Meditsina 1971; 5(6):48–52.
5. Dyhre-Poulsen P, Laursen AM. Programmed electromyographic activity and negative incremental muscle stiffness in monkeys jumping downward. J Physiol 1984; 350:121–36.
6. Fregly AR, Graybiel A. An ataxia test battery not requiring the use of rails. Pensacola, FL: Naval Aerospace Medical Institute/ NASA 1966; No. NAMI-985. NASA R-93.
7. Gurfinkel V. The mechanisms of postural regulation in man. Soviet Sci Rev, Sect F: Physiol Gen Biol Rev 1994; 7(5):59–89.
8. Homick JL, Reschke MF. Postural equilibrium following exposure to weightless space flight. Acta Otolaryngol 1977; 83:455–64.
9. Kenyon RV, Young LR. M.I.T./Canadian vestibular experiments on the Spacelab-1 mission: 5. Postural responses following exposure to weightlessness. Exp Brain Res 1986; 64:335–46.
10. Layne CS, McDonald PV, Pruett CJ, et al. Preparatory postural control after space flight. Soc Neurosci Abstr 1995; 21:138.
11. Ljung, L. System Identification Toolbox User's Guide. Natick, MA: The MathWorks, Inc. 1993.
12. Martin TP, Edgerton VR, Grindeland RE. Influence of spaceflight on rat skeletal muscle. J Appl Physiol 1988; 65:2318–25.
13. McDonald PV, Basdogan C, Bloomberg JJ, Layne CS. Lower limb kinematics during treadmill walking after space flight: implications for gaze stabilization. Exp Brain Res 1996; 112:325.
14. McKinley PA, Smith L. Visual and vestibular contributions to prelanding EMG during jump-downs in cats. Exp Brain Res 1983; 52:439–48.
15. McMahon TA, Cheng GC. The mechanics of running: how does stiffness couple with speed? J Biomechan 1990; 23 (Suppl. 1):65–78.
16. Melvill Jones G, Watt DGD. Observations on the control of stepping and hopping movements in man. J Physiol 1971; 219:709–27.
17. Nashner LM, Berthoz A. Visual contribution to rapid motor responses during postural control. Brain Res 1978; 150:403–7.
18. Newman DJ, Jackson DK, Bloomberg JJ. Altered astronaut lower limb and mass center kinematics in downward jumping following space flight. Exp Brain Res 1997; 117:30–42.
19. Newman DJ, Schultz KU, Rochlis JL. Closed loop estimator based model of human posture following reduced gravity exposure. AIAA J Guidance, Control, and Dynamics.; 1996; 19:1102–8.
20. Paloski WH, Black FO, Reschke MF, et al. Vestibular ataxia following shuttle flights: effects of transient microgravity on otolith-mediated sensorimotor control of posture. Am J Otology 1993; 14(1):9–17.
21. Parker DE, Reschke MF, Arrot AP, Lichtenberg BK. Otolith tilt-translation reinterpretation following prolonged weightlessness: implications for preflight training. Aviat Space Environ Med 1985; 56:601–6.
22. Reschke MF, Anderson DJ, Homick JL. Vestibulo-spinal response modification as determined with the H-reflex during the Spacelab-1 flight. Exp Brain Res 1986; 64:367–79.
23. Thompson HW, McKinley PA. Effect of visual perturbations in programming landing from a jump in humans. Soc Neurosci Abstr 1988; 14:66.
24. Watt DGD, Money KE, Bondar RL, et al. Canadian medical experiments on Shuttle Flight 41-G. Can Aeronaut Space J 1985; 31:215–26.
25. Watt DGD, Money KE, Tomi LM. M.I.T./Canadian vestibular experiments on the Spacelab-1 mission: 3. Effects of prolonged weightlessness on a human otolith-spinal reflex. Exp Brain Res 1986; 64:308–15.
26. Wilkinson L. SYSTAT. The system for statistics. Evanston, IL: SYSTAT, Inc. 1989.
27. Young J, Chandler RF, Snow CC, et al. Anthropometric and mass distribution characteristics of the adult female. Oklahoma City, OK: Federal Aviation Administration Civil Aeromedical Institute 1983; No. FAA-AM-83–16.
28. Young LR, Oman CM, Watt DGD, et al. M.I.T./Canadian vestibular experiments on the Spacelab-1 mission: 1. Sensory adaptation to weightlessness and readaptation to one-g: an overview. Exp Brain Res 1986; 64:291–8.